

Fabrication of TiB₂ particulate reinforced magnesium matrix composites by two-step processing method

Yan Wang, Hui-Yuan Wang, Kun Xiu, Hong-Ying Wang, Qi-Chuan Jiang *

The Key Laboratory of Automobile Materials of Ministry of Education and Department of Materials Science and Engineering, Jilin University at Nanling Campus, No. 142 Renmin Street, Changchun 130025, PR China

Received 22 July 2005; accepted 22 November 2005
Available online 9 December 2005

Abstract

The magnesium matrix composites reinforced with 2, 5 and 7.5 wt.% fine TiB₂ (~7 μm) particulates were fabricated by a novel two-step processing method, i.e. adding a TiB₂–Al compact mixed with fine TiB₂ and Al powders to magnesium melt and using a semi-solid slurry stirring technique. The microstructure and properties such as porosity, hardness and wear resistance of the composites were investigated. The distribution of fine TiB₂ particulates is relatively homogeneous throughout the Mg matrix. As compared with as-cast AZ91, the hardness and wear resistance of the Mg composite was higher and increased with increasing of TiB₂ content, but the porosity of the composites was relatively higher and increased with increasing of TiB₂ content.

© 2005 Elsevier B.V. All rights reserved.

Keywords: Magnesium; Composite; TiB₂; Wear

1. Introduction

Due to the increasing demand on lightweight materials in automotive and aerospace applications, Mg and its alloys gain increasing attention in the scientific community and in the industry [1,2]. Their moderate mechanical and physical properties, however, limit their proliferation in demanding applications such as structural and functional materials. The incorporation of suitable ceramic particulates can compensate for many of these limitations, leading to engineering materials with high specific properties, improved wear resistance and lower coefficients of thermal expansion [3,4].

A number of manufacturing techniques have been developed to produce ceramic particulate reinforced Mg metal matrix composites (MMCs), such as stir casting [5,6], mechanical alloying (MA) [7], powder metallurgy (P/M) [1,8,9], squeeze cast [10], disintegrated melt deposition (DMD) [3,11], infiltration [4,12] and self-propagating high-temperature synthesis (SHS) [13,14]. Compared with other methods, stir casting

costs as little as one-third to one-tenth for mass production [15] and therefore the stir casting is the most economical and easily adoptable method [16]. In addition, Mg composites fabricated by this method can form a near net shape microstructure by using conventional foundry techniques [17]. In conventional stir casting process [5,6,17], the particulates were usually added onto Mg melt surface and the particulates were then entrapped at the vortex formed by the force of stirring. However, some reactant products on the surface of the Mg melt were also engulfed in the Mg melt, which may lead to higher porosity in the composite.

Among the various ceramic reinforcements in particulate reinforced Mg composites, SiC is the most widely used because of its relatively better wettability and stability in Mg melt [16]. In recent years, TiC and B₄C have received more attention in the Mg composites [4,14,18,19]. Titanium diboride (TiB₂), possessing outstanding features such as high melting point (2790 °C), high hardness (33 GPa), high modulus (530 GPa) and low density (4.451 g/cm³) [20,21], is another potential reinforcement in Mg composites. However, investigation on TiB₂ particulate reinforced magnesium MMCs is rather limited [9,13,22]. Wang et al. [13] adopted SHS method to fabricate in situ particulate reinforced Mg composites, but the

* Corresponding author. Tel./fax: +86 431 509 4699.

E-mail address: jiangqc@mail.jlu.edu.cn (Q.-C. Jiang).

unfavorable brittle Al_3Ti phase with large size was also formed in the Mg composites, which may degrade plasticity of the composites.

The purpose of this study is to investigate the feasibility of the fabrication of Mg MMCs reinforced with different fraction of fine TiB_2 particulates by using two-step processing method, i.e. adding a TiB_2 –Al compact mixed with fine TiB_2 and Al powders to magnesium melt and using a semi-solid slurry stirring technique. The microstructures, porosity, hardness and wear resistance of the composites are also discussed.

2. Experimental

Pure Al powder (99.0% purity, $\sim 29 \mu\text{m}$) and TiB_2 particulates (96.5% purity, $\sim 7 \mu\text{m}$) in proportion of 1:1 (wt.%) were mixed by ball milling for 8 h in a stainless steel container. The mixtures were then mechanically pressed into cylindrical pre-forms with the same diameter (20 mm) and different thickness (26, 62 and 98 mm, respectively) at pressures ranging from 75 to 80 MPa. The Al powder was used to prepare the compact for the purpose that Al is a main alloy element of AZ91 and the compact prepared with Al can easily be incorporated into the matrix melt due to its relatively high density. Each compact with about 72% theoretical density was dried in a vacuum oven at 100°C for 1 h to remove water. The Mg matrix was prepared by melting commercially pure Mg, Al and Zn according to the chemical compositions of Mg-9 pctAl-1 pct Zn alloy AZ91. About 500 g matrix was heated at 750°C and held at that temperature for 10 min in an electric resistance furnace containing a graphite crucible under SF_6/CO_2 protective atmosphere, as shown in Fig. 1. And then the dried TiB_2 –Al compact was quickly added into the magnesium melt and held at that temperature until the compact was dissolved. When the melt cooled

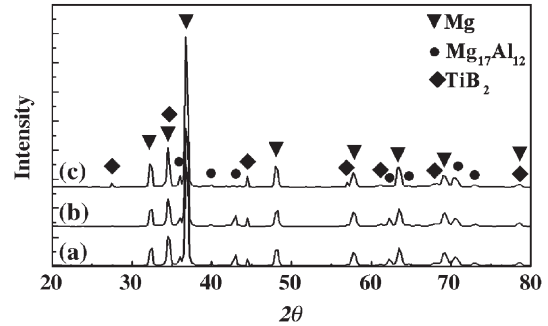


Fig. 2. XRD patterns of various amounts of TiB_2 particulate reinforced AZ91 composites fabricated by two-step processing method. (a) 2 wt.% $\text{TiB}_2/\text{AZ91}$, (b) 5 wt.% $\text{TiB}_2/\text{AZ91}$ and (c) 7.5 wt.% $\text{TiB}_2/\text{AZ91}$.

down just below the liquidus, stirring was carried out for 20 min. The placement of mechanical stirrer and the stirring velocity must be carefully controlled to avoid the engulfment of reaction products on the melt. And then the composite slurry was heated at 730°C and then was poured into a pre-heated steel mould with 55 mm diameter and 150 mm height.

The theoretical density of Mg composite was calculated using the rule of mixtures [23]. The real densities for the as-cast AZ91 and composite were measured using Archimedes principle. The details of density measurement were given elsewhere [9]. In addition, the abrasive wear testing was performed under 25 N load using a pin-on-disc apparatus. The as-cast AZ91 and composite were used as pin materials with 6 mm diameter and 12 mm height, and 1000 grit SiC abrasive papers (corresponding to $15 \mu\text{m}$ abrasive particles) were used as the counterface.

Microstructure and phase analyses of the composite were investigated by using scanning electron microscopy (SEM) (Model JSM-5310, Japan) equipped with energy-dispersive

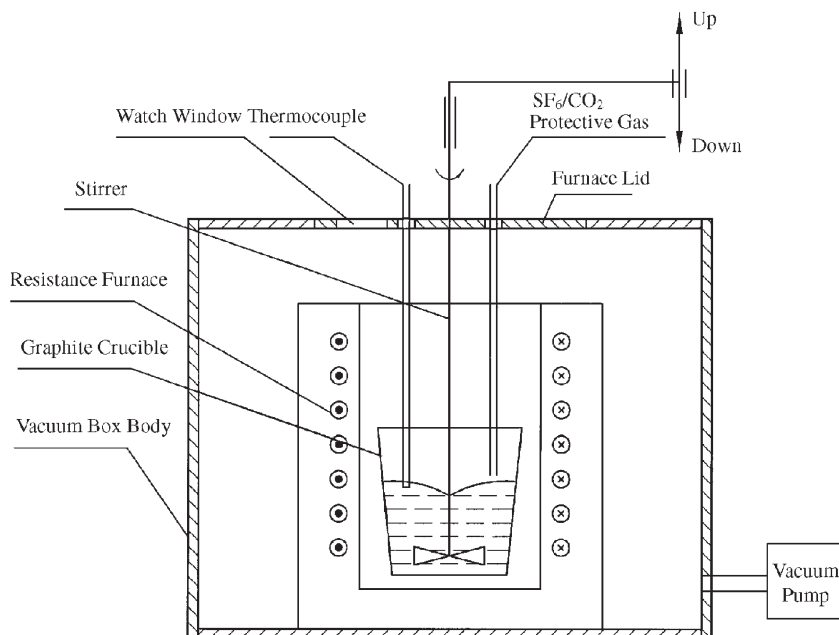


Fig. 1. Schematic diagram of an apparatus for fabricating particulate reinforced Mg composites by two-step processing method.

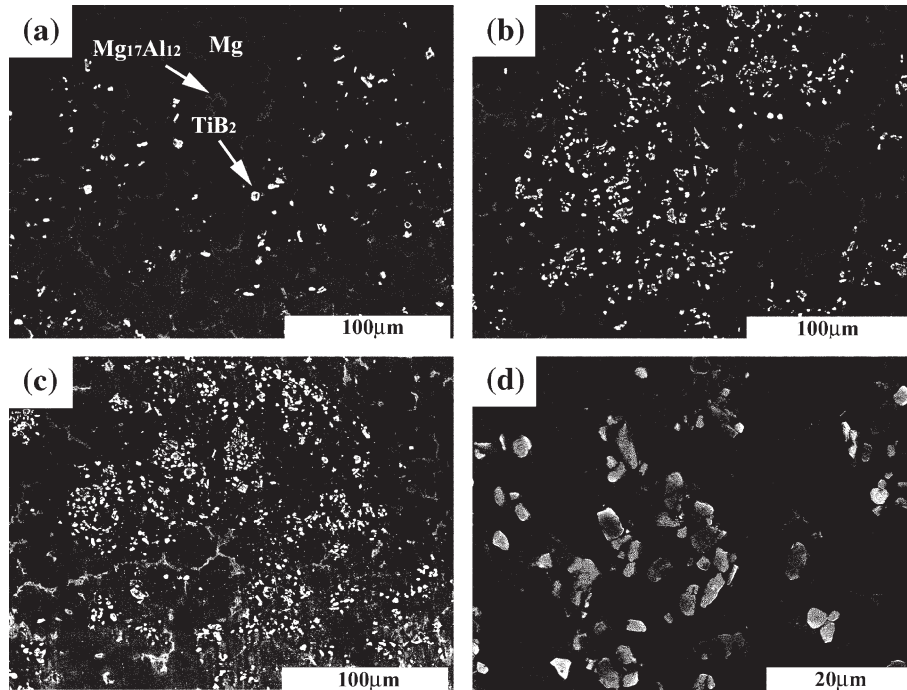


Fig. 3. SEM microstructures of various amounts of TiB_2 particulate reinforced AZ91 composites fabricated by two-step processing method. (a) 2 wt.% $\text{TiB}_2/\text{AZ91}$, (b) 5 wt.% $\text{TiB}_2/\text{AZ91}$, (c) 7.5 wt.% $\text{TiB}_2/\text{AZ91}$ and (d) high magnification SEM micrograph of the Mg composite reinforced with 7.5 wt.% TiB_2 .

spectrum (EDS) (Model Link-Isis, Britain) and X-ray diffraction (XRD) (Model D/Max 2500PC Rigaku, Japan).

3. Results and discussion

3.1. Microstructure

Figs. 2 and 3 show the XRD patterns and SEM micrographs of the 2, 5 and 7.5 wt.% TiB_2 particulate reinforced Mg MMCs fabricated by two-step processing method, respectively. From the XRD results, the composites consist of Mg, TiB_2 and $\text{Mg}_{17}\text{Al}_{12}$, indicating that TiB_2 is relatively stable in magnesium. EDS analysis identified that the dark phase in Fig. 3 is magnesium, while the gray phase is $\text{Mg}_{17}\text{Al}_{12}$ and the white phase is TiB_2 (marked in Fig. 3(a)). It is interesting to note that the distribution of $\text{Mg}_{17}\text{Al}_{12}$ was not homogeneous in the Mg matrix (see Fig. 3(b) and (c)) and the investigation on the reason for this is continuing in our group. It is well known that a key challenge in the processing of particulate reinforced composites is to homogeneously distribute the reinforcement phases to achieve a defect-free microstructure, and the finer the particulates, the more difficult the homogeneous distribution of particulate. High magnification SEM micrograph (as shown in Fig. 3(d)) shows that the TiB_2 particulate is fine ($\sim 7 \mu\text{m}$) and irregular, and in the mean time there were some submicron TiB_2

particulates in the composites. Therefore, some agglomeration of TiB_2 particulate can be observed, and the general distribution of TiB_2 is relatively homogeneous throughout the Mg matrix (in Fig. 3(a)–(c)). The stirring during a semi-solid state can help break the gas layer and perhaps oxide layers as well and spread the liquid metal onto surface of TiB_2 particulates, thus helping to achieve good wettability [24]. On the other hand, the semi-solid stirring is usually considered to help the increase in the apparent viscosity, which inhibits particulates settling and floating, and helps the separation of the cluster of TiB_2 particulates [25]. Therefore, the semi-solid stirring is feasible for fabrication of fine TiB_2 particulate reinforced Mg composite.

3.2. Porosity

In accordance with the theoretical density, real density of each composite, the porosity of each material can be calculated according to the equation: $P = 1 - \rho_a / \rho_t$ where P is the porosity of the material, ρ_a is the real density and ρ_t is the theoretical density. It assumed that the real density of as-cast AZ91 is taken as the theoretical density of as-cast AZ91.

Table 1 shows the theoretical density, real density and porosity of the as-cast AZ91 and as-cast Mg composites fabricated by two-step

Table 1
The theoretical densities, real densities and porosities of the as-cast AZ91 and as-cast composites reinforced with 2, 5 and 7.5 wt.% TiB_2

Material	Theoretical density (g/cm^3)	Real density (g/cm^3)	Porosity (vol.%)
AZ91	–	1.81	–
2 wt.% $\text{TiB}_2/\text{AZ91}$	1.84	1.82	0.656
5 wt.% $\text{TiB}_2/\text{AZ91}$	1.86	1.84	1.176
7.5 wt.% $\text{TiB}_2/\text{AZ91}$	1.90	1.86	2.134

Table 2

The hardness and volume wear rate of the as-cast AZ91 and as-cast composites reinforced with 2, 5 and 7.5 wt.% TiB_2

Material	Hardness (HB)	Volume wear rate ($10^{-10} \text{ m}^3/\text{m}$)	Increment (%) ^a
AZ91	62	13.48401	–
2 wt.% $\text{TiB}_2/\text{AZ91}$	74	11.14763	21.0
5 wt.% $\text{TiB}_2/\text{AZ91}$	80	9.42015	43.1
7.5 wt.% $\text{TiB}_2/\text{AZ91}$	82	7.91921	70.3

^a The data in this column refer to wear resistance percentage change with respect to as-cast AZ91.

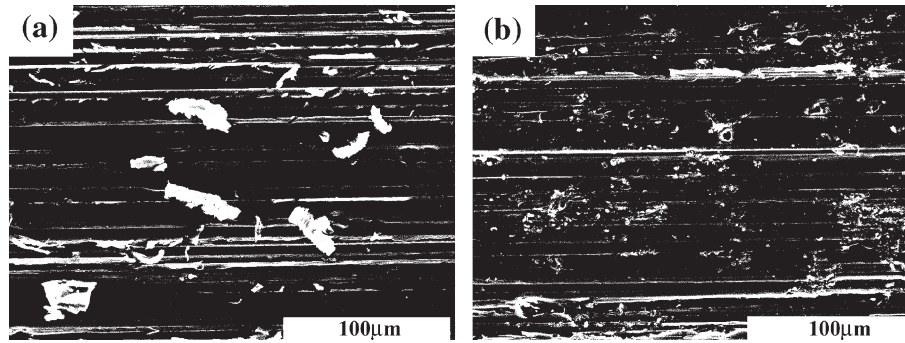


Fig. 4. SEM micrographs of the worn surfaces of (a) as-cast AZ91 and (b) 5 wt.% TiB₂/AZ91 composite fabricated by two-step processing method.

processing method. Compared with as-cast AZ91, the porosity of the composite is slightly higher. When the particulates were dispersed in Mg melt, the apparent viscosity of the composite melt increased, and thus the composite melt fluidity decreased during the pouring and solidification [26]. Therefore, the porosity of the composite is higher than that of as-cast AZ91. During the incorporation, the TiB₂-Al compact spontaneously sank to the bottom of the crucible due to the inertia of its falling and its density being higher than that of the Mg melt, rather than float on the melt surface. Due to the addition of TiB₂ in form of TiB₂-Al compact, stirring in semi-solid state, and proper controlling stir parameter, very little reactant products on the Mg melt surface were engulfed into the composite slurry during the stirrings. And the fluidity of the composite decreased slightly, and therefore, the porosity of the composite is slightly higher than that of as-cast AZ91.

In addition, as TiB₂ content in the composite increased, the apparent viscosity of the composite slurry increased and the fluidity decreased. Hence, the porosity of the composite increased with increasing of the TiB₂ particulate content.

3.3. Hardness and wear resistance

Hardness values and volumetric wear rates of the as-cast AZ91 and TiB₂/AZ91 composites are listed in Table 2. It is clear that the hardness of TiB₂/AZ91 composites is higher than that of as-cast AZ91. This can be attributed primarily to (a) the presence of harder TiB₂ particulate in the magnesium matrix and (b) a higher constraint to the localized matrix deformation during indentation as a result of the presence of TiB₂. It is interesting to note that the increase of hardness of the composite reinforced with 7.5 wt.% TiB₂ is relatively lower compared with those of the composites reinforced with 2 and 5 wt.% TiB₂. The reason for this difference is that the composite reinforced with 7.5 wt.% TiB₂ possessed relative high porosity compared with the other two composites.

It can be seen from Table 2 that the as-cast AZ91 exhibits the highest volume loss due to its relatively low hardness and that the addition of only 2 wt.% TiB₂ to AZ91 matrix leads to an obvious reduction in volume wear rate. The volumetric wear rates of the composites decreased obviously with the increasing of TiB₂ content from 2 to 7.5 wt.%. The abrasive wear resistance is defined as the inverse of volume loss [27]. Therefore, the increased wear resistance of Mg MMCs reinforced with TiB₂ is attributed to the increase of the hardness of the composite and to the slow wear of TiB₂ particulate.

Fig. 4(a) and (b) shows the SEM micrographs of the worn surfaces of as-cast AZ91 and 5 wt.% TiB₂/AZ91 composite fabricated by two-step processing method, respectively. Apparently, the worn surface of as-cast AZ91 is rough because of the presence of distinct grooves; however, that of the composite has a relatively smooth appearance.

The abrasive wear behavior of as-cast AZ91 and the Mg composites is a microploughing and microcutting abrasion and the TiB₂ particulates in Mg matrix produce an excellent effect on resisting the abrasive particulate entering into the matrix, bearing loads, strengthening matrix and preventing deformation. The pull-out particulate is not observed during sliding and TiB₂ particulate remains stable on the worn surface under the ploughing action. This implies a strong interfacial bonding between the TiB₂ particulate and magnesium matrix.

4. Conclusions

- (1) The magnesium matrix composites reinforced with 2, 5 and 7.5 wt.% fine TiB₂ particulates were successfully fabricated by two-step processing method. Microstructural characterization showed that the distribution of fine TiB₂ particulates is relatively homogeneous throughout the Mg matrix due to the incorporation of TiB₂ into molten Mg in form of TiB₂-Al compact and stirring in semi-solid state.
- (2) Although the porosity of the composites was higher than that of as-cast AZ91, the increase of porosity of the composites is relatively small due to adopting of two-step processing method and proper controlling stir parameter.
- (3) The hardness and wear resistance of the composites were higher compared with as-cast AZ91 and increased with increasing of TiB₂ content.

Acknowledgements

This work is supported by The National Natural Science Foundation of China (No. 50371030 and 50531030) and the project 985-Automotive Engineering of Jilin University.

References

- [1] S.F. Hassan, M. Gupta, Mater. Sci. Eng. A392 (2005) 163–168.
- [2] S. Spigarelli, D. Ciccarelli, E. Evangelista, Mater. Lett. 58 (2004) 460–464.
- [3] C.Y.H. Lim, D.K. Leo, J.J.S. Ang, M. Gupta, Wear 259 (2005) 620–625.
- [4] A. Contreras, V.H. Lopez, E. Bedolla, Scr. Mater. 51 (2004) 249–253.
- [5] A. Luo, Metall. Mater. Trans., A Phys. Metall. Mater. Sci. 26 (1995) 2445–2455.
- [6] R.A. Saravanan, M.K. Surappa, Mater. Sci. Eng., A Struct. Mater.: Prop. Microstruct. Process. 276 (2000) 108–116.
- [7] L. Lu, K.K. Thong, M. Gupta, Compos. Sci. Technol. 63 (2003) 627–632.

- [8] H. Ferkel, B.L. Mordike, *Mater. Sci. Eng., A Struct. Mater.: Prop. Microstruct. Process.* 298 (2001) 193–199.
- [9] H.Y. Wang, Q.C. Jiang, Y. Wang, B.X. Ma, F. Zhao, *Mater. Lett.* 58 (2004) 3509–3513.
- [10] A.R. Vaidya, J.J. Lewandowski, *Mater. Sci. Eng., A Struct. Mater.: Prop. Microstruct. Process.* 220 (1996) 85–92.
- [11] S.F. Hassan, M. Gupta, *Metall. Trans., A, Phys. Metall. Mater. Sci.* 36 (2005) 2253–2258.
- [12] Q. Dong, L.Q. Chen, M.J. Zhao, J. Bi, *Mater. Lett.* 58 (2004) 920–926.
- [13] H.Y. Wang, Q.C. Jiang, X.L. Li, F. Zhao, *J. Alloys Compd.* 366 (2004) L9–L12.
- [14] H.Y. Wang, Q.C. Jiang, X.L. Li, J.G. Wang, *Scr. Mater.* 48 (2003) 1349–1354.
- [15] M.K. Surappa, *J. Mater. Process. Technol.* 63 (1997) 325–333.
- [16] H.Z. Ye, X.Y. Liu, *J. Mater. Sci.* 39 (2004) 6153–6171.
- [17] M.C. Gui, J.M. Han, P.Y. Li, *Mater. Sci. Technol.* 20 (2004) 765–771.
- [18] C. Badini, *Mater. Sci. Eng., A Struct. Mater.: Prop. Microstruct. Process.* 157 (1992) 53–61.
- [19] Q.C. Jiang, H.Y. Wang, B.X. Ma, Y. Wang, F. Zhao, *J. Alloys Compd.* 386 (2004) 513–519.
- [20] K.L. Tee, L. Lu, M.O. Lai, *J. Mater. Process. Technol.* 89–90 (1999) 513–519.
- [21] S.C. Tjong, G.S. Wang, *Adv. Eng. Mater.* 6 (2004) 964–968.
- [22] M.A. Matin, L. Lu, M. Gupta, *Scr. Mater.* 45 (2001) 479–486.
- [23] M. Merola, *Mater. Sci. Eng., A Struct. Mater.: Prop. Microstruct. Process.* 214 (1996) 181–185.
- [24] W. Zhou, Z.M. Xu, *J. Mater. Process. Technol.* 63 (1997) 358–363.
- [25] M.C. Flemings, *Metall. Trans., A, Phys. Metall. Mater. Sci.* 22 (1991) 957–981.
- [26] A. Mortensen, I. Jin, *Inter. Mater. Rev.* 37 (1992) 101–128.
- [27] S.C. Tjong, K.C. Lau, *Compos. Sci. Technol.* 59 (1999) 2005–2013.